Evidence for a New Magnetic Field Scale in $CeCoIn_5$

I. Sheikin,[1] H. Jin,[2] R. Bel,[2] K. Behnia,[2] C. Proust,[3] J. Flouquet,[4] Y. Matsuda,[5] D. Aoki,[4] and Y. Ōnuki[6]

[1]*Grenoble High Magnetic Field Laboratory (CNRS), BP 166, 38042 Grenoble, France*
[2]*Laboratoire de Physique Quantique (CNRS), ESPCI, 10 Rue de Vauquelin, 75231 Paris, France*
[3]*Laboratoire National des Champs Magnétiques Pulsés (CNRS), BP 4245, 31432 Toulouse, France*
[4]*DRFMC/SPSMS, Commissariat à l'Energie Atomique, F-38042 Grenoble, France*
[5]*Department of Physics, University of Kyoto, Kyoto 608-8502, Japan*
[6]*Graduate School of Science, Osaka University, Toyonaka, Osaka 560-0043, Japan*

(Received 26 May 2005; published 24 February 2006)

The Nernst coefficient of $CeCoIn_5$ displays two distinct anomalies in magnetic field. The feature detected at $H_K \sim 23$ T is similar to what is observed in $CeRu_2Si_2$ at $H_m = 7.8$ T where a metamagnetic transition occurs. In $CeCoIn_5$, new frequencies are observed in de Haas–van Alphen oscillations when the field exceeds 23 T where the Dingle temperature decreases by about 30%. Based on the Nernst coefficient anomalies, the magnetic phase diagram of $CeCoIn_5$ is revised.

DOI: 10.1103/PhysRevLett.96.077207 PACS numbers: 75.30.Kz, 71.27.+a, 73.43.Nq

Heavy-fermion (HF) compounds [1] display a dazzling variety of physical phenomena. The "non-Fermi-liquid" behavior emerging in the vicinity of a magnetic quantum critical point (QCP), associated with a continuous phase transition at zero temperature, has recently attracted much attention [2]. The case of the HF superconductor $CeCoIn_5$ [3] is intriguing. Magnetic field alters the normal-state properties of this compound in a subtle way. In zero field, $CeCoIn_5$ displays neither a T^2 resistivity nor a T-linear specific heat (standard features of a Landau Fermi liquid) down to the superconducting (SC) transition. When superconductivity is destroyed by pressure [4] or magnetic field [5,6], the Fermi-liquid state is restored. In the latter case, the field-tuned QCP identified in this way is pinned to the upper critical field, $H_{c2}(0)$ of the SC transition [7,8], which becomes first order at very low temperatures [9]. This is unexpected because quantum criticality is often associated with the destruction of magnetic order. The possible existence of a magnetic order with a field scale close to H_{c2} and accidentally hidden by superconductivity has been speculated [6].

Comparing $CeCoIn_5$ with the well-documented case of $CeRu_2Si_2$ [10,11] is instructive. In $CeRu_2Si_2$ a metamagnetic (MM) transition occurs at $H_m = 7.8$ T: the magnetization jumps from $0.6\mu_B$ to $1.2\mu_B$ in a narrow window ($\Delta H_m = 0.04$ T at the $T = 0$ limit). The passage from an antiferromagnetically (AF) correlated state below H_m to a polarized one dominated by local fluctuations above is accompanied by a sharp increase of the quasiparticle mass in the vicinity of H_m which is thus akin to a field-tuned QCP. New de Haas–van Alphen (dHvA) frequencies were detected above H_m [12].

We report on two sets of studies which indicate that the effect of the magnetic field on the normal-state properties of $CeRu_2Si_2$ and $CeCoIn_5$ shares common features. The measurements of the Nernst coefficient and dHvA effect provide compelling evidence that close to $H_K \sim 23$ T the electronic properties are modified. Therefore, at the $T = 0$ limit, $CeCoIn_5$ appears to display at least two distinct field scales.

Single crystals of $CeCoIn_5$ were grown by a self-flux method. Thermoelectric coefficients were measured using a one-heater-two-thermometer setup. dHvA measurements were performed using a rotating cantilever torquemeter.

We begin by presenting the field dependence of the Nernst coefficient of $CeRu_2Si_2$, which demonstrates the sensitivity of this probe. The upper panel of Fig. 1 shows the field dependence of the Nernst signal ($N = \frac{E_y}{\nabla_x T}$) in $CeRu_2Si_2$. Around the MM transition field, $H_m = 7.8$ T, N abruptly changes sign. The field dependence of the Nernst signal presents additional structure. The lower panel of Fig. 1 shows the field dependence of the dynamic Nernst coefficient, $\nu = \frac{\partial N}{\partial B}$, at 2.2 K. It presents two anomalies just below and above H_m: a sharp minimum at $\sim$8.2 T and a smaller maximum at 7 T. The inset shows the temperature dependence of these two anomalies which closely follow the lines of the phase diagram of $CeRu_2Si_2$. These are crossover lines which represent anomalies detected by specific heat [13,14] and thermal expansion [15] measurements.

The case of $CeRu_2Si_2$ shows how sensitively the Nernst signal probes metamagnetism. This is presumably due to its relationship with the energy dependence of the scattering rate [the so-called Mott formula: $\nu = \frac{\pi^2 k_B^2 T}{3m}(\frac{\partial \tau}{\partial \epsilon})|_{\epsilon=\mu}$]. Let us now focus on the case of $CeCoIn_5$. The first study of the Nernst effect in this compound found a very large zero-field Nernst coefficient emerging below $T^* \sim 20$ K [16]. Below T^*, resistivity is linear in temperature [3,5,17], the Hall coefficient is anomalously large [17,18], the thermoelectric power is anomalously small [16], and the electronic specific heat rises rapidly with decreasing temperature [3,6]. All these anomalous properties gradually disappear when a magnetic field is applied. In particu-

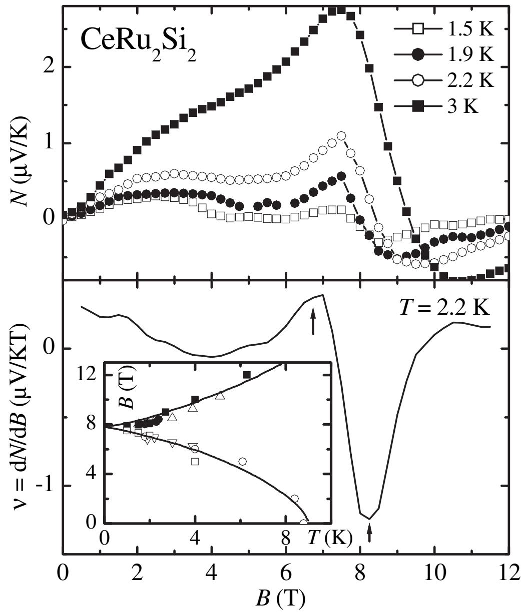

FIG. 1. Upper panel: field dependence of the Nernst signal in $CeRu_2Si_2$ for selected temperatures. Lower panel: the Nernst coefficient, defined as the derivative of the signal at $T = 2.2$ K. The arrows show the position of a maximum and a minimum close to H_m. The inset shows the position of these anomalies (triangles) in the B-T plane compared to those detected by previous studies of thermal expansion [solid and empty circles [15]] and specific heat [solid and empty squares [13,14]].

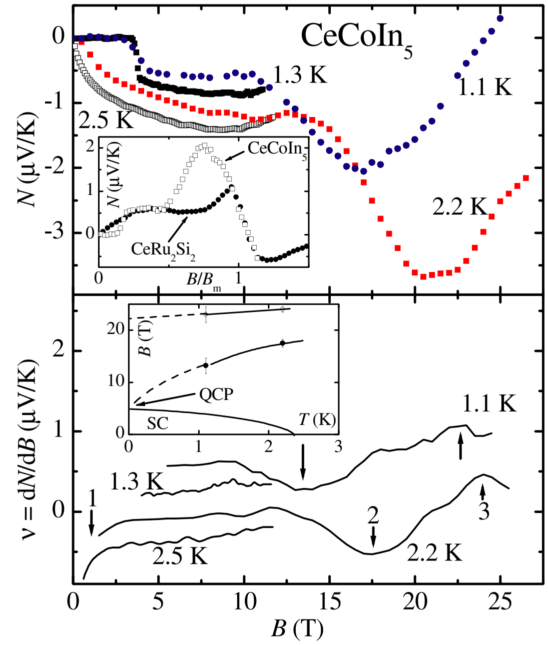

FIG. 2 (color online). Upper panel: field dependence of the Nernst signal in $CeCoIn_5$ for different temperatures. The inset compares the field dependence of the Nernst coefficient as a function of a normalized field in the two compounds. Lower panel: the dynamic Nernst coefficient obtained by taking the derivative of N. The curves for 1.1 K, 1.3 K, and 2.5 K were shifted by a constant value. Arrows identify the three anomalies discussed in the text. A sketch of the B-T phase diagram based on these anomalies is shown in the inset.

lar, the giant Nernst effect also gradually fades away in the presence of a moderate magnetic field [16].

The field dependence of the Nernst coefficient in the 12–28 T field range reveals new features emerging at even higher magnetic fields. The B-T phase diagram of the system is apparently more complicated than previously suggested, and the field associated with the emergence of the Fermi liquid close to $H_{c2}(0)$ ($\sim$5 T) is not the only relevant field scale for $CeCoIn_5$.

Figure 2 presents the field dependence of the Nernst signal, N, and its dynamic derivative, ν, in a magnetic field up to 28 T along the c axis. At the onset of superconductivity ($T = 2.2$ K), N rises rapidly as a function of field at low fields. Thus, its derivative, ν, is large (anomaly no. 1). With the application of a moderate magnetic field, the Nernst signal saturates and therefore ν becomes very small. Above 13 T, N suddenly increases again, rapidly reaches a maximum, and then decreases. The field dependence of N at $T = 1.1$ K follows the same pattern with all field scales shifted to lower values. While opposite in sign, the Nernst signal of the two compounds displays a similar field dependence. This can be seen by plotting the absolute value of N for both compounds as a function of B/B_m, with B_m (22.5 T at 1.1 K for $CeCoIn_5$ and 7.9 T at 2.2 K for $CeRu_2Si_2$) corresponding to a magnetic field at which the Nernst signal drastically decreases and changes sign. As seen in the inset of the upper panel of Fig. 2, the comparison establishes the existence of a field scale at 22.5 T in $CeCoIn_5$ in close analogy to the one already detected in $CeRu_2Si_2$. A lower-field scale associated with an opposite and somewhat smaller change in the magnitude of N can also be detected. These two features lead to anomalies (no. 2 and no. 3) of opposite sign in plots of $\nu(B)$ similar to what was observed in $CeRu_2Si_2$.

However, contrary to the case of $CeRu_2Si_2$, the two distinct field scales in $CeCoIn_5$ do not tend to merge at the $T = 0$ limit. The lower-field anomaly (no. 2) lies close to the line already identified by the resistivity measurements [5]. At $T \to 0$, this line is very close to $H_{c2}(0)$ ($\sim$5 T for $B \parallel c$). The high-field anomaly (no. 3) identifies another (almost horizontal) line in the B-T plane and yields a second field scale ($\sim$ 23 T). A sketch of the B-T phase diagram of $CeCoIn_5$ is shown in the inset of Fig. 2.

High-resolution dHvA measurements provide further evidence for the existence of the second distinct field scale at $H_K \sim 23$ T in $CeCoIn_5$. Figure 3 shows the torque signal at $T = 40$ mK as a function of field applied close to the c axis. The anomalies observed at around 5 T correspond to the suppression of superconductivity. There are no other anomalies at higher field. This is in contrast with $CePd_2Si_2$, where a MM transition at 9 T was established by torque measurements [19]. However, an emergence of a new

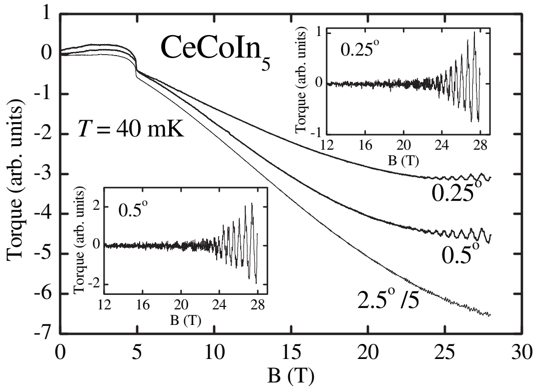

FIG. 3. Field dependence of the magnetic torque in $CeCoIn_5$ observed at 40 mK for three orientations of the magnetic field close to the c axis. The insets show the high-field oscillatory torque signal after subtracting the nonoscillating background.

dHvA frequency is clearly seen above ~23 T and becomes more obvious after subtracting the nonoscillating background (insets of Fig. 3). Fourier spectra of the dHvA oscillations indicate that other frequencies also appear above 23 T. This is another evidence of the second distinct field scale at 23 T.

Figure 4 shows a comparison of the Fourier spectra of the dHvA oscillations below and above 23 T for B at 0.5° and 2.5° from the c axis, the two orientations for which the effective masses were determined. The frequencies F_i, $i = 1 \dots 5$ are observed both below and above 23 T and are in line with those found in the previous dHvA studies performed at lower fields [20–23]. The frequencies F_2, F_3, F_4, and F_5 correspond to quasi-two-dimensional Fermi surfaces (FS) that are well accounted for by the itinerant f-electron band structure calculations [21,22].

Above 23 T, two new frequencies F_a and F_b appear in the oscillatory spectrum with B at 0.5° from the c axis [Fig. 4(b)]. Two more frequencies, F_c and F_d, are observed above 23 T applied at 2.5° [Fig. 4(d)]. Neither of the new frequencies was observed in the previous lower-field dHvA studies. The average effective masses over the field range 23–28 T corresponding to the new frequencies are strongly enhanced being about $33m_0$, $49m_0$, $18m_0$, and $24m_0$ for F_a, F_b, F_c, and F_d, respectively. The effective masses of all the frequencies are field dependent. However, those of the frequencies observed both below and above 23 T do not show any anomalies at that field. The frequencies F_a and F_b are field dependent themselves; F_a decreases and F_b increases with field. This rules out the possibility of F_b being the second harmonic of F_a though $F_b \approx 2F_a$. The frequency F_4 also decreases with field, but does not show any anomaly at 23 T.

The frequency F_a might correspond to one of the closed orbits of the 15-electron band of the $4f$-itinerant band structure calculations [21,22]. The other frequencies observed above 23 T are difficult to reconcile with either $4f$-itinerant or $4f$-localized calculations [22,24]. On the other hand, F_b is very close to the frequency A observed in $CeRhIn_5$ just above its critical pressure $P_c = 2.35$ GPa [25] and in $CeCoIn_5$ under pressure [26]; F_c and F_d are located in the same frequency range where several new frequencies were observed in $CeRhIn_5$ just below P_c [25].

The frequencies F_a and F_b exist only over a small angular range close to the c axis and might be due to a magnetic breakdown. This is not the case for the frequencies F_c and F_d which survive over a wide angular range between the [001] and [100] directions. The angular dependence of F_c is very similar to those of F_2, F_3, and F_4; the angular dependence of F_d is analogous to that of F_5. Therefore, F_c and F_d are likely to originate from quasi-two-dimensional FS.

Figure 5 shows the Dingle plot for several dHvA frequencies; the field dependence of the corresponding effective masses was taken into account. The slope of the lines determine the Dingle temperature given by $T_D = \frac{\hbar}{2\pi k_B \tau}$, where τ is quasiparticle scattering lifetime. T_D is a measure

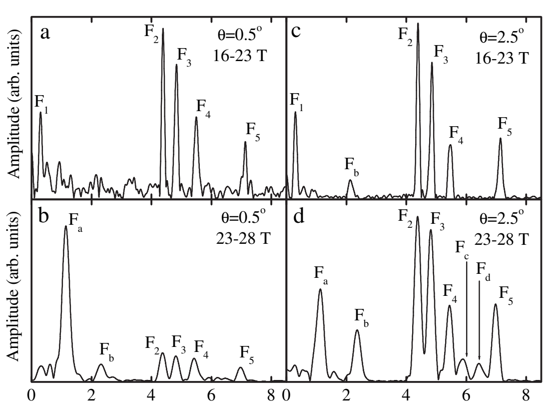

FIG. 4. Fourier spectra of the dHvA oscillations below [(a),(c)] and above [(b),(d)] 23 T are compared for B at 0.5° [(a),(b)] and 2.5° [(c),(d)] from the c axis. The new frequencies are denoted by F with a letter index.

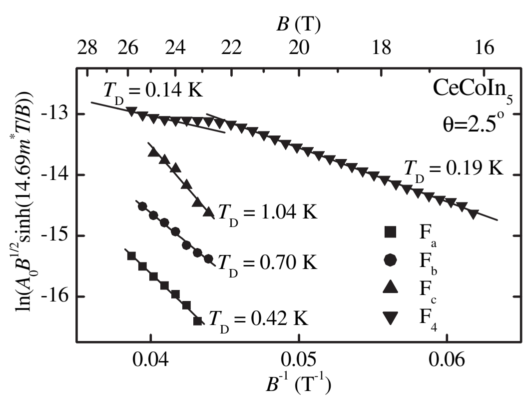

FIG. 5. Dingle plot for the branches F_a, F_b, F_c, F_d, and F_4 with B at 2.5° from the c axis. The Dingle temperatures of the other branches are difficult to estimate because of either very high effective masses or very close frequencies.

of the degree of scattering of the quasiparticles. The slope of the Dingle plot for the F_4 branch changes around 23 T corresponding to a change of T_D from 0.19 K below that field to 0.14 K above it. A similar change of the Dingle plot slope was observed at ~40 T in $YbAl_3$ where it was argued to arise from the renormalization of the quasiparticle states by the field [27]. A strong anomaly in the Dingle plot was also observed in $CeRu_2Si_2$ in the immediate vicinity of the MM transition [28].

The Dingle temperatures of F_a, F_c, and F_d are higher than that of F_4 (Fig. 5). If these Dingle temperatures also increase by about 30% below 23 T, the corresponding oscillations would be beyond the detection level of present measurements. Therefore, we cannot distinguish whether the new frequencies observed above 23 T result from a topological change of the FS or from a change of T_D. High-field specific heat measurements suggest ~50% decrease of the low temperature specific heat coefficient at 28.5 T compared to the zero-field value, thus favoring the latter scenario [29]. However, such measurements were only reported for 20 and 28.5 T above 1.5 K.

Thus, two independent sets of evidence point to the existence of a new field scale in $CeCoIn_5$ at 23 T. We also note that a temperature scale of ~20 K, (comparable to the energy associated with a field of 23 T) marks most of the zero-field properties of the heavy-electron fluid in $CeCoIn_5$. However, what occurs in the case of $CeCoIn_5$ does not appear as a MM transition [22] (defined as a jump in the magnetization).

In HF systems, the interplay between magnetic intersite interactions with a characteristic energy scale E_m and local Kondo fluctuations with a characteristic energy $k_B T_K$ changes with the application of a magnetic field. When the associated Zeeman energy becomes comparable with one of the characteristic energy scales, the balance between these two interactions is modified. This defines two characteristic field scales, H_m and H_K, given by $g\mu H_m \simeq E_m$ and $g\mu H_K \simeq k_B T_K$. Furthermore, an external magnetic field adds a ferromagnetic (F) component to the existing AF one. The field redistribution among different AF, F, and Kondo components depends on the type of the local anisotropy (Ising, planar, or Heisenberg character) and the lattice deformation produced by magnetostriction. In this context, an important difference between $CeRu_2Si_2$ and $CeCoIn_5$ is that the susceptibility in the latter compound is much less anisotropic. $CeRu_2Si_2$, with a magnetic anisotropy of 15 compared to 2 in $CeCoIn_5$, is much closer to an Ising-like system. In $CeCoIn_5$, magnetic field seems to induce a QCP at $H_{c2}(0)$ [5,6]. Because of the weak magnetic anisotropy of $CeCoIn_5$ H_m should vanish at the field-induced QCP [1] as was observed in $YbRh_2Si_2$ [30] and $CeNi_2Ge_2$ [31]. For $CeCoIn_5$, this may explain the existence of a large field domain between H_{c2} and H_K where AF and F correlations compete. The change of the correlations nature at $H_K \sim 23$ T is strongly supported by the observed change of the Dingle temperature.

While the field-induced evolution of the magnetic interactions in $CeCoIn_5$ does not occur through a MM transition as in $CeRu_2Si_2$, a similar behavior of the Nernst signal in both compounds is not surprising as ν is proportional to the energy derivative of the scattering rate.

In conclusion, we have demonstrated the existence of another field scale in $CeCoIn_5$ besides H_{c2}. The new characteristic field $H_K \sim 23$ T is marked by an anomaly in the Nernst signal similar to that observed at the MM field of $CeRu_2Si_2$. Contrary to $CeRu_2Si_2$, in $CeCoIn_5$ the two distinct field scales remain widely separated at the $T = 0$ limit. New dHvA frequencies are observed above 23 T where the Dingle temperature becomes lower. This suggests an important modification of the quasiparticle scattering.

This work was supported as a part of the ICENET project by ANR (ANR-05-BLAN-0055-02) and by the EC program "Transnational Access - Specific Support Action" (Contract No. RITA-CT-2003-505474).

[1] For a review, see J. Flouquet, cond-mat/0501602.
[2] G. R. Setwart, Rev. Mod. Phys. **73**, 797 (2001).
[3] C. Petrovic *et al.*, J. Phys. Condens. Matter **13**, L337 (2001).
[4] V. A. Sidorov *et al.*, Phys. Rev. Lett. **89**, 157004 (2002).
[5] J. Paglione *et al.*, Phys. Rev. Lett. **91**, 246405 (2003).
[6] A. Bianchi *et al.*, Phys. Rev. Lett. **91**, 257001 (2003).
[7] E. D. Bauer *et al.*, Phys. Rev. Lett. **94**, 047001 (2005).
[8] F. Ronning *et al.*, Phys. Rev. B **71**, 104528 (2005).
[9] A. Bianchi *et al.*, Phys. Rev. Lett. **89**, 137002 (2002).
[10] P. Haen *et al.*, J. Low Temp. Phys. **67**, 391 (1987).
[11] J. Flouquet *et al.*, Physica (Amsterdam) **B319**, 251 (2002).
[12] H. Aoki *et al.*, Phys. Rev. Lett. **71**, 2110 (1993).
[13] Y. Aoki *et al.*, J. Magn. Magn. Mater. **177-181**, 271 (1998).
[14] H. P. van der Meulen *et al.*, Phys. Rev. B **44**, 814 (1991).
[15] C. Paulsen *et al.*, J. Low Temp. Phys. **81**, 317 (1990).
[16] R. Bel *et al.*, Phys. Rev. Lett. **92**, 217002 (2004).
[17] Y. Nakajima *et al.*, J. Phys. Soc. Jpn. **73**, 5 (2004).
[18] M. F. Hundley *et al.*, Phys. Rev. B **70**, 035113 (2004).
[19] I. Sheikin *et al.*, Phys. Rev. B **67**, 094420 (2003).
[20] D. Hall *et al.*, Phys. Rev. B **64**, 212508 (2001).
[21] R. Settai *et al.*, J. Phys. Condens. Matter **13**, L627 (2001).
[22] H. Shishido *et al.*, J. Phys. Soc. Jpn. **71**, 162 (2002).
[23] A. McCollam *et al.*, Phys. Rev. Lett. **94**, 186401 (2005).
[24] N. Harrison *et al.*, Phys. Rev. Lett. **93**, 186405 (2004).
[25] H. Shishido *et al.*, J. Phys. Soc. Jpn. **74**, 1103 (2005).
[26] H. Shishido *et al.*, J. Phys. Condens. Matter **15**, L499 (2003).
[27] T. Ebihara *et al.*, Phys. Rev. Lett. **90**, 166404 (2003).
[28] M. Takashita *et al.*, J. Phys. Soc. Jpn. **65**, 515 (1996).
[29] J. S. Kim *et al.*, Phys. Rev. B **64**, 134524 (2001).
[30] W. Tokiwa *et al.*, J. Magn. Magn. Mater. **272-276**, E87 (2004).
[31] P. Gegenwart *et al.*, J. Low Temp. Phys. **133**, 3 (2003).